

Toward Physical Modeling of Laser Welding: Thermophysics Revisited

A. Cramer · A. Lange · Yu. Plevachuk ·
V. Sklyarchuk

Received: 19 May 2008 / Accepted: 15 November 2008 / Published online: 16 December 2008
© Springer Science+Business Media, LLC 2008

Abstract Experimental determination of the thermophysical properties (thermal and electrical conductivity, viscosity, and surface tension) of lithium iodide was carried out in the temperature range starting slightly above the melting point and extending to about 950 K. These measurements are motivated by the search for a transparent substance, the Prandtl number Pr of which approaches or is even less than unity, and which shows a stable Marangoni effect with respect to potential contamination of the melt. Such a combination of material properties is mandatory in the attempt of physical modeling of laser welding processes where optical access to the bulk of the fluid is needed to measure the flow field. In an extension to these basic studies, the electrical conductivity and the influence of the admixture of other iodides on Pr was also studied.

Keywords Electrical conductivity · Lithium iodide · Prandtl number · Surface tension · Thermal conductivity · Viscosity

A. Cramer
Department of Magnetohydrodynamics, Forschungszentrum
Dresden-Rossendorf, P. O. Box 510119, 01314 Dresden, Germany

A. Lange (✉)
Institute of Surface and Manufacturing Technology,
Universität Dresden, 01062 Dresden, Germany
e-mail: adrian.lange@tu-dresden.de

Yu. Plevachuk · V. Sklyarchuk
Department of Metal Physics, Ivan Franko National University,
8 Kyrylo and Mephodiy St., 79005 Lviv, Ukraine

1 Motivation and Review of Related Work

1.1 Liquid Metal Model Experiments

An everlasting and notorious problem in the physical modeling of industrially relevant flows in the fields of metallurgy, and here in particular in the sub-division of welding, or in crystal growth, is the choice of an appropriate model fluid. From the point of view of hydraulics, it is fully justifiable to do experiments on water instead of trying, for example, to acquire data from a hot and aggressive steel melt. Quite a lot of investigations rely on a single underlying similarity criterion, which is the Reynolds number $Re = uL/\nu$ in the case of mere hydraulics. Among the physical properties, only the kinematic viscosity ν is affected to such an extent as it can not be compensated with the experimentally adjustable parameters u and L (characteristic velocity and length).

As soon as other phenomena enter the problem, probably the most simple of which is the presence of temperature gradients ΔT , the overall physics of the system is likely to change. It is not a problem with respect to physical modeling that one is now concerned with both heat and mass transfer. That fluid flow may be caused by ΔT is unproblematic also. Serious difficulties in reliable modeling will, however, arise from the retroaction of the fluid flow on the temperature distribution, the latter being potentially the sole source of motion. This means that a second dimensionless group, which somehow accounts for the ratio between convected and diffused heat, joins Re . Because the realm of fluid mechanics is beyond the scope of this article, only the result is given: to model nonisothermal processes comprising fluid flow, it is mandatory to have fair agreement of both Re and the Prandtl number $Pr = \nu/\chi$ between the real facility and the experiment, respectively. Here, χ denotes the thermal diffusivity.

Since ultrasonic Doppler velocimetry (UDV) [1]¹ has developed almost in parallel with liquid metal model experiments [3], quite a lot of physical modeling on industrially relevant flows has hitherto concentrated on metallic melts having a low melting point. In most applications, the ternary GaInSn alloy, which is a liquid at room temperature, has replaced mercury for safety reasons. With the typical low Prandtl number of liquid metals ($Pr < 0.1$), it fulfills the above mentioned prerequisites for nonisothermal flows and thus seems, in conjunction with its low vapor pressure and convenient manageability, an ideal candidate for physical modeling.

1.2 Importance of Thermocapillarity for Welding

The drawback of room-temperature liquid metals, and this continues to be true for all alloys with melting points in a reduced temperature range such as SnPb or PbBi, is that all of them are prone to oxidation. This deficiency is a key for welding; whereas bulk flow phenomena may be nicely studied for low melting-point metals, flow driven

¹ For an overview on measuring techniques for liquid metal flows, see [2].

by thermocapillary forces, as is predominant in welding, must not be modeled with such materials. It is well known that the Marangoni effect is very sensitive in that even an oxide layer of the thickness of a few molecules, and more so any surface active agent, might change the convection behavior. We have found only two groups [4,5] that managed to observe Marangoni convection at a metallic surface under the condition of a significantly lowered temperature. Closer examination of this work shows that such experiments are extremely difficult to perform, and, moreover, are strictly limited with respect to adaptability to any technical process of interest. Thus, for an important class of industrial processes including welding, liquid metal model experiments will fail if they do not consider the existence of a third dimensionless group, which is the Marangoni number $Ma = -\partial\gamma/\partial T \cdot \Delta TL/\eta\chi$. $\partial\gamma/\partial T$ denotes the derivative of the surface tension with respect to temperature and η is the dynamic viscosity.

When browsing through available literature to determine the state of the art in meaningful model experiments on welding, one inevitably discovers a huge amount of publications claiming to be motivated by metallurgical or crystal growth processes. None of them is referred to here; it is instead left to the reader to consider whether substances such as silicon oils, ethanol, acetone, or other organic substances, invariably exhibiting a value of the Prandtl number many times over unity, are an appropriate means regarding the claim. What substances remain after gathering the information above, considering that liquid metals will not work for Marangoni convection as a result of unpredictable corrosion?

1.3 Why Molten Salts Might be the Favorite Medium to Model Welding

In general, the idea to use molten salts as worthy of imitation in materials processing is not new [6,7]. In 1980, Sadoway and Szekely [6] proposed, to our knowledge for the first time, the use of eutectic LiCl–KCl as a viable option to model the flow in a metallurgical operation. Albeit concerned with the problem of electromagnetic stirring, this article comprises some of the features that are also important in the present work. Molten salts are relatively stable with respect to alterations of surface tension by contamination, and they are transparent; the authors report on laser Doppler anemometric measurements. Nonetheless, this article exhibits, representatively for quite a lot of applied research, a symptomatic deficiency: it was admitted that some of the material properties are estimated from similar substances, and from our existing knowledge, they were unreliable. Whereas in [6] the material property of main interest was the electrical conductivity; Koziol and Sadoway moved toward thermophysics while proposing the same material [7]. With their statement, (quote taken from the abstract), “. . . use of physical models, such as water and organic liquids, . . . suffer from the fact that their Prandtl numbers are too high.” these authors address exactly the problem of meaningful modeling of the actual heat transfer described above. However, the Prandtl number of LiCl–KCl is 6, and thus higher than $Pr_{(\text{CH}_3)_2\text{CO}} = 4$ of acetone, which is an organic fluid. The target is $Pr \leq 1$: not until Pr reaches unity does the convective heat transport lose predominance.

In a series of three publications [8–10], Limmaneevichitr and Kou report on model experiments that are claimed to have been especially adapted to welding. The pool shape resembled that of a weld pool, and localized heat input at the surface was established by a laser beam. At first sight, these experiments seem to be a meaningful contribution to the community of welding as these authors used two model fluids, a gallium melt with $Pr = 2.3 \times 10^{-2}$ and sodium nitrate with $Pr = 9.1$, with the intention to study also the influence of the Prandtl number. Closer examination reveals that the outcome of these experiments is limited. It is proved beyond doubt that liquid gallium exhibits an almost no slip boundary condition at its surface due to a dense oxide layer. That is to say, it does not show any Marangoni convection rendering the experiments carried out on NaNO_3 as not appropriate to model any metallurgical process involving temperature gradients. Therefore, all these experiments, including those on surface active agents, show only general trends.

From our present knowledge of material properties of molten salts, it is indicated that there are only two candidates that may fulfill the requirement $Pr \leq 1$. Both are not easily manageable because of their relatively high melting points and chemical aggressiveness. Despite the fact that the properties of potassium chloride are known better, the present work was carried out in favor of lithium iodide because it requires a significantly lower mechanistic effort to have it melted.

2 Measuring Methods

2.1 Electrical Conductivity

The electrical conductivity was determined according to Ohm's law, which means contacting the sample, passing a current through it, and measuring the voltage drop. As it is state of the art to use four wires to improve accuracy, such a method where the current is supplied via one pair of wires and the voltage is measured with a second pair was also employed in the present work. Tungsten–rhenium 5/20 thermocouples were used in alternate action. In their general mode of operation, they were used for temperature measurements, whereas one limb of the thermocouples was used as the electrode to sense the electric potential. All electrical connections to the melt sample were established with graphite electrodes mounted on the wall of the measuring cell. This cell was a cylinder 2.5 mm in inner diameter and 50 mm in height made from ceramic boron nitride (BN). The cylinder was oriented vertically so as to have the current feeding electrodes at the bottom and close to the top, and the sensing electrodes in between in the cylinder envelope.

A furnace provided a temperature distribution, the inhomogeneity of which was not worse than 0.3 K over the extension of the experimental cell in the temperature range up to 1000 K. The measurement uncertainty of the absolute temperature was about 1.5 K. The thermal expansion of BN is negligible and is not expected to have a detectable influence on the data. To protect the graphite and the wires from oxidation, the experiments were performed under an argon atmosphere. All constructive components employed had a purity of 99.999 %, whereas the sample composition was accurate within 0.02 mass%. The resultant error of the electrical conductivity measurements is

about 2%. Further details of this method and its experimental realization are found in [11].

2.2 Viscosity

Measurements of the viscosity were carried out with a computer-controlled oscillating-cup viscometer (cf. [12]). Samples of about 30 g contained in sealed cylindrical crucibles of 14 mm in inner diameter were heated to temperatures of about 800 K. As in the case of the determination of the electrical conductivity, temperatures were sensed with a W–Re 5/20 thermocouple and found to vary not more than 0.3 K within the furnace. For acquisition acquirement of the data series, the thermocouple was placed directly below the crucible. The composition of the LiI was also here accurate to 0.02 mass%. Each sample was weighed before and after the measurements to ensure that no loss of mass occurred. A protective helium atmosphere under a negligible excess pressure of about 0.02 MPa to 0.03 MPa sufficed for this experiment.

Using Roscoe's equation [13], the dynamic viscosity $\eta(T)$ can be calculated from the logarithmic decrement and the period of the oscillations. The uncertainty of the viscosity measurements is estimated to be about 3%.

2.3 Thermal Conductivity

An experimental arrangement based on the steady-state concentric cylinder method [14] was used for measurements of the thermal conductivity $\lambda(T)$. The apparatus was composed of two coaxial cylinders separated by a gap, into which the melt was poured. A concentric hole was drilled in the inner cylinder so as to provide the space for an internal heater, which was made from molybdenum wire wound on an alumina form. At the open end, a cover was sealed onto the cell with a heat-resistant compound. The outermost part of the three-section furnace consisted of a molybdenum wire wound on a BN form. It produced the lower over-all temperature level while its upper and lower sections permitted the control of the temperature field over the height of the apparatus. The inner heater produced the necessary temperature gradient in the melt layer. Again, W–Re 5/20 thermocouples were used, two of them placed in the body of the inner cylinder to allow examination of the temperature distribution over the radius of the apparatus.

The coefficient of thermal conductivity can be calculated from the formula for the heat transfer in a cylindrical layer. The design of the apparatus assured minimization of the heat leakage and of convection within the molten sample. The resultant uncertainty of thermal conductivity measurements was about 7%.

2.4 Surface Tension

The surface tension was measured in the temperature range between the melting point T_m and 1000 K using a “large drop” method. This technique is a modification of the sessile drop method and allows overcoming problems typically arising from the asym-

metry of a large sessile drop [15]. Two advantages of the modification over the sessile drop technique are: (i) the large axisymmetric meniscus may be employed with both wetting and nonwetting systems and (ii) the drop enlargement allows reducing the experimental uncertainty by almost one order of magnitude. A circular crucible having its upper circumferential edge chamfered acute-angled was overfilled with fluid so as to accomplish an axisymmetric meniscus, the diameter of which exceeded that of the crucible and which raises above the rim. To avoid oxidation of the sample, the experiments were performed in an atmosphere of 90 % Ar + 10 % H₂ after initially evacuating the working volume of the chamber.

The temperature was measured with the W–Re 5/20 thermocouple located near the specimen while it was maintained within ± 1 K. A CCD camera and computer-controlled equipment were used for determination of the drop parameters. Based on the Laplace–Young equation, the surface tension $\gamma(T)$ was calculated by Kozakevitch's method [16]. All surface tension data were obtained with an uncertainty of about 0.5 %.

3 Results and Discussion

3.1 Melting Temperature

The first measurements of T_m of LiI brought to our attention were conducted by Janz [17] and Janz et al. [18]. These authors published a T_m value of about 722 K. After repetition of the measurements more than 10 years later, the same principal investigator—Janz et al. [19]—reported a T_m value of about (742 ± 3) K, which differs by 20 K from the previous one. Because such a difference is significant and to ensure that the most recent value might be seen as a correction, it was also mandatory to evaluate T_m for LiI within the present work. Although no explicit determination of the melting point was done, the current measurements clearly support the latter of the references mentioned above. This is most evidently seen in the dynamic viscosity η depicted in Fig. 1. $T = 739$ K was the lowest temperature for which it was possible to measure a viscosity value in agreement with its temperature dependence. It is the lower limit of the interval reported in [19].

3.2 Viscosity

The sole measurement published on the viscosity of LiI of which we are aware is provided by Janz [17]. Since viscosity is known to decrease exponentially with temperature, this author suggested a fit in the form,

$$\eta(T) = A \exp \left\{ \frac{E}{RT} \right\} \quad (1)$$

in the temperature range $730 \text{ K} \leq T \leq 920 \text{ K}$ investigated here. R is the universal gas constant having a value of $1.986 \text{ cal} \cdot \text{K}^{-1} \cdot \text{mol}^{-1}$. As can be seen in Fig. 1, the present measurement (Table 1) fits nicely to this exponential law with $A = 115.1 \times 10^{-3} \text{ mPa} \cdot \text{s}$ and $E = 4423.0 \text{ cal} \cdot \text{mol}^{-1}$. The good agreement to the data supplied by Janz serves

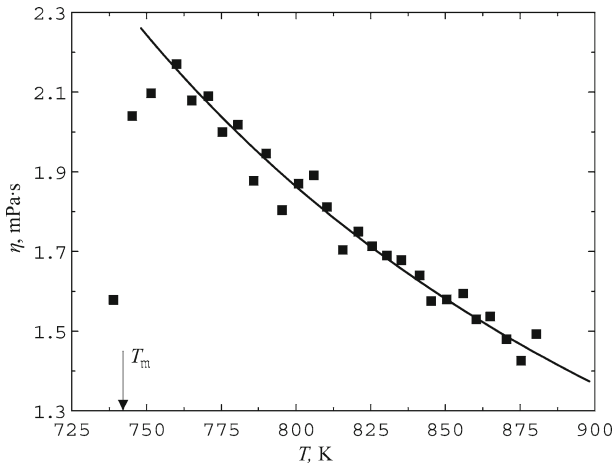


Fig. 1 Variation of the dynamic viscosity with temperature. Squares are the measured values and solid line is a fit according to Eq. 1, in which the values for the three lowest temperatures (the salt is not completely molten) are ignored

as a sound basis for calculation of the temperature dependence of the Prandtl number as shown below.

3.3 Thermal Conductivity

In Fig. 2, the thermal conductivity λ is plotted. The measured data (Table 2) in the temperature range 775 K to 955 K suggest a linear dependence on temperature, a least-squares fit of which yields

$$\lambda(T) = -0.62 \left[\text{W} \cdot \text{m}^{-1} \cdot \text{K}^{-1} \right] + 1.82 \times 10^{-3} T \left[\text{W} \cdot \text{m}^{-1} \cdot \text{K}^{-2} \right]. \quad (2)$$

It is to be considered that λ_{LiI} was measured for the first time in the present work, and thus a gap is filled since this thermal property is needed in the calculation of the Prandtl number. The most recent and comprehensive investigation on iodides comprises salts with sodium, potassium, rubidium, and cesium, but not lithium [20].

At this stage, it seems appropriate to compare the new result in terms of its influence on Pr with the other iodides. Because λ enters the denominator of Pr , as high values as possible is desirable. Figure 3 contrasts the thermal conductivities measured in [20] to that of LiI. The outcome of the comparison has two aspects that one might term striking. First, λ_{LiI} increases with temperature whereas the thermal conductivity of all other iodides decreases. Second, the absolute value of λ_{LiI} surpasses the others by a factor of three to four. Another seemingly meaningful comparison would be that of LiI with other lithium halides. Unfortunately, there are only few data available. With the exception of lithium fluoride, for which only a single value from a secondary source exists, the thermal conductivity of LiI is the highest among the halides. As can be seen

Table 1 Measured dynamic viscosity η as a function of temperature T

T (K)	η (mPa · s)
739.04	1.578
745.31	2.040
751.58	2.097
760.00	2.170
765.11	2.079
770.67	2.090
775.37	2.000
780.53	2.018
785.87	1.877
790.02	1.946
795.35	1.804
800.88	1.870
806.00	1.891
810.39	1.812
815.66	1.704
820.86	1.750
825.47	1.713
830.43	1.690
835.23	1.678
841.36	1.640
845.25	1.576
850.47	1.580
856.00	1.595
860.35	1.530
865.10	1.537
870.43	1.480
875.32	1.426
880.43	1.493

in Fig. 4, the dependence of λ on temperature is weaker than that of LiI, and in the case of the only systematic measurement on LiCl, is negative.

3.4 Surface Tension

Since thermocapillarity, i.e., the derivative of the surface tension γ with respect to temperature T , is the predominant force driving convection in a weld pool, $\partial\gamma/\partial T$ is probably the most important thermophysical property in the present work. From [19], one of the most important publications on molten salts related to this work, it is immediately seen that difficult to access Russian literature [22,23] is referenced. Fortunately, the authors of [23] published the surface tension data on LiI again [24]. Identical values from [19,23,24]

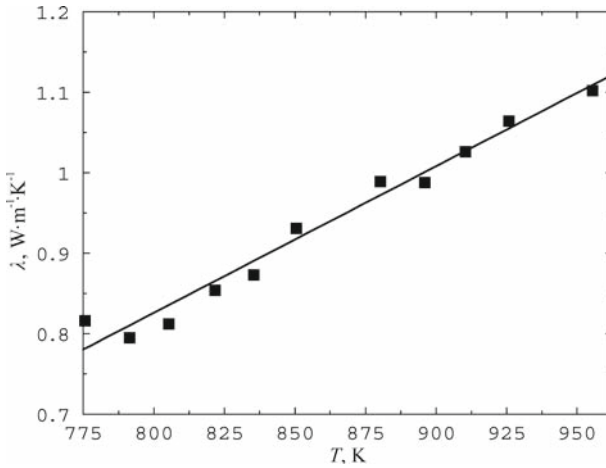


Fig. 2 Variation of thermal conductivity with temperature. *Squares* denote measured results, and *line* represents a linear fit (Eq. 2)

Table 2 Measured thermal conductivity λ as a function of temperature T

T (K)	λ ($\text{W} \cdot \text{m}^{-1} \cdot \text{K}^{-1}$)
775.50	0.816
790.74	0.795
805.65	0.812
821.25	0.854
835.25	0.873
850.47	0.931
880.40	0.989
896.02	0.988
910.44	1.026
925.86	1.064
955.47	1.102

$$\gamma(T) = 140.7 \left[\text{mN} \cdot \text{m}^{-1} \right] - 5.65 \times 10^{-2} T \left[\text{mN} \cdot \text{m}^{-1} \cdot \text{K}^{-1} \right]. \quad (3)$$

may indicate that the data in [22] were ignored in [19] as a coincidental agreement of four digits in the absolute value and another three digits in the derivative is unlikely to occur. This means that, to the best of our knowledge, only one source for the surface tension of LiI is provided in the literature. Although the measurement error is estimated to be as small as 0.5%, no further information about the two values of γ_0 and $\partial\gamma/\partial T$ are given in [24]. Because of the importance of surface tension, this situation of very limited information prompted us to contact the authors. The communication [25] revealed that γ had been measured between 758 K and 1,084 K with a mean square

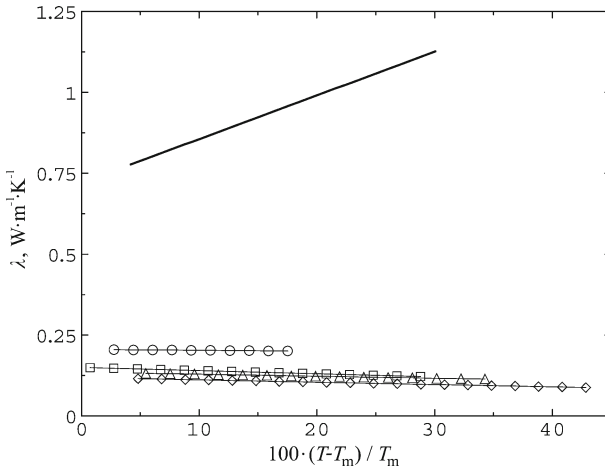


Fig. 3 Comparison of the dependence of thermal conductivity on temperature among iodides. Temperatures on the abscissa are in percentage relative to the melting temperature T_m of the respective iodide. *Solid line* represents the present measurement on LiI, data for NaI (*circle*), KI (*square*), RbI (*triangle*), and CsI (*diamond*) are taken from [20]

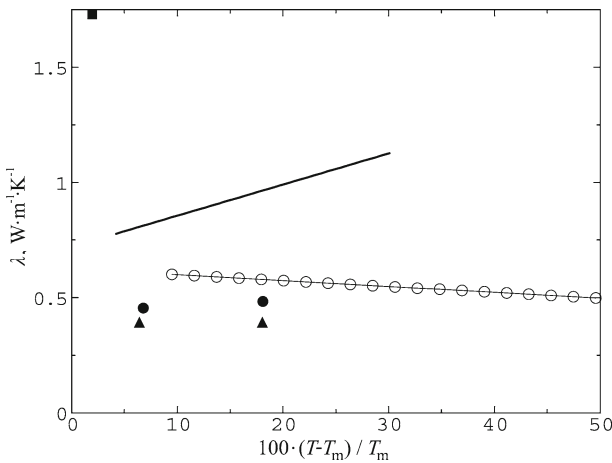


Fig. 4 Dependence of the thermal conductivity of lithium halides on temperature. As in Fig. 3, temperatures are given in percent above melting point. *Solid line* shows the present measurements for LiI. Data for LiF (*square*) and for LiBr (*triangle*) are taken from [19], those for LiCl (*black circle*, *white circle*) are to be found in [19] and [21], respectively

deviation of $2 \text{ mJ} \cdot \text{m}^{-2}$, which indicates a little larger potential error than that given in [24].

A comparison between the results of the present work and those in [24] is shown in Fig. 5. The linear fit of the measured values (Table 3) in the temperature range 760 K to 980 K yields

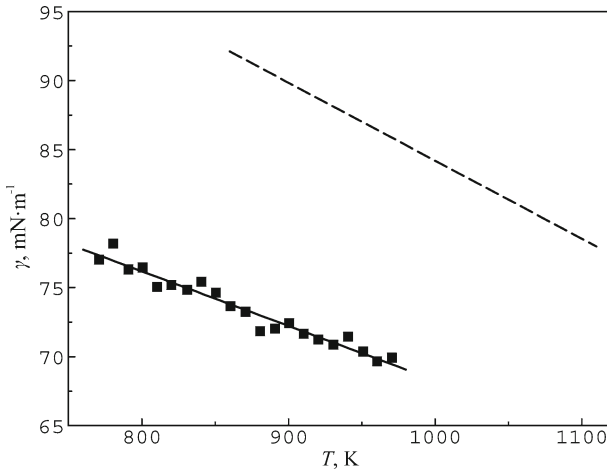


Fig. 5 Variation of the surface tension γ with temperature. The fit of the present measurements (*solid line*) indicates a constant coefficient $\frac{\partial\gamma}{\partial T} = -3.95 \times 10^{-5} \text{ N} \cdot \text{m}^{-1} \cdot \text{K}^{-1}$. A discussion of the obvious discrepancy with previous data from Smirnov and Stepanov [24] (*dashed line*) is provided in the text

$$\gamma(T) = 107.8 \left[\text{mN} \cdot \text{m}^{-1} \right] - 3.95 \times 10^{-2} T \left[\text{mN} \cdot \text{m}^{-1} \cdot \text{K}^{-1} \right]. \quad (4)$$

As neither the large sessile drop method described in Sect. 2.4 nor the maximum bubble pressure technique employed by Smirnov and Stepanov might be expected to show large measuring errors, one is concerned with a systematic deviation here.

Let us assume for the moment that both methods measure the actual value of γ of the salt melt within the errors estimated above, say 1%. Then, consequently, γ has to be different according to Eqs. 4 and 3 as a result of the experimental conditions under which it is measured. In the maximum bubble pressure technique, the surface is freshly created immediately prior to that instant in time when the measurement is taken. The large sessile drop method, however, is inherently slow. It takes quite a lot of time from the preparation of the sample, then melting and heating it to the desired temperature, until the final measurement can be performed. That several temperatures were measured in the present investigation within one experimental run while the values of γ still nicely fit a systematic model clearly indicates that the overall system is somehow in equilibrium.

This has to be seen in conjunction with what is said about the prerequisites for meaningful physical modeling above, namely, a stable Marangoni effect. The surface tension of the new-born surface may indeed be most accurately measured with the maximum bubble pressure method, but it is prone to degrade over a period of time. An unstoichiometric evaporation of elementary iodine is assumed to be a possible reason of the decrease of γ . As this undesired effect can not be completely avoided, one is likely concerned with the lower values of γ in Eq. 4 in any modeling of a welding process based on LiI.

Table 3 Measured surface tension γ as a function of temperature T

T (K)	γ (mN · m ⁻¹)
770.83	77.03
780.50	78.20
790.77	76.33
800.55	76.47
810.44	75.05
820.16	75.20
830.83	74.84
840.72	75.42
850.44	74.63
860.44	73.64
870.77	73.26
880.61	71.84
890.94	72.04
900.61	72.44
910.55	71.65
920.44	71.24
930.66	70.87
940.55	71.45
951.05	70.37
960.50	69.66
970.61	69.94

3.5 Prandtl Number

For a determination of the dimensionless Prandtl number,

$$Pr = \frac{\nu}{\chi} = \eta \frac{c_p}{\lambda}, \quad (5)$$

where $\chi = \lambda/(\rho c_p)$, ρ is the density, c_p is the heat capacity which has to be known in addition to the measured values of η and λ . According to [19], the heat capacity does not depend on temperature in the range between 742 and 802 K. Thus, it is assumed that the variation of c_p is also small in the range extending to temperatures a little higher for which both measurements of η and λ are available within the present work. At least, the dependence of c_p is so small compared to the dependences of η and λ on T that it can be neglected in the calculation of Pr . This assumption is strongly supported by the findings of Murgulescu and Telea [26], who investigated the heat capacity of four different iodides and did not find any significant dependence of c_p on T [26]. Using the value of $c_p = 472.36 \text{ J} \cdot \text{Kg}^{-1} \cdot \text{k}^{-1}$ [19] in Eq. 5, a plot of the variation of Pr with T can be made. As can be seen in Fig. 6 and Table 4, the decrease of Pr with

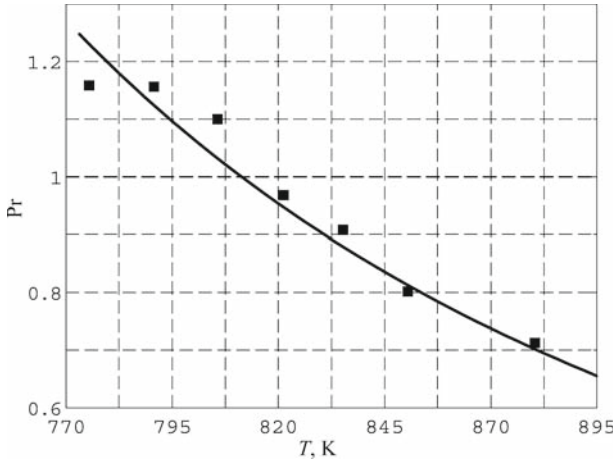


Fig. 6 Prandtl number of LiI based on the fits in Eqs. 1 and 2 and on $c_p = 472.36 \text{ J} \cdot \text{Kg}^{-1} \cdot \text{k}^{-1}$

Table 4 Prandtl number Pr for selected temperatures T

T (K)	Pr
775.50	1.158
790.74	1.156
805.65	1.100
821.25	0.968
835.25	0.908
850.47	0.802
880.40	0.713

increasing T is significant thanks to the steep increase of $\lambda(T)$. Most noteworthy, the goal of having $Pr \leq 1$ where the diffusion and convection become of equal importance is reached at not too high temperatures. In the experimentally manageable range of higher temperatures, the diffusivity dominated regime may be studied for the first time with a transparent substance.

3.6 Electrical Conductivity and Salt Mixtures

Although electronic properties are somewhat removed from the scope of the present paper, the electrical conductivity σ is worth considering for two reasons. One of these is the interesting question of how LiI performs against LiCl–KCl proposed in [6] for the use in physical modeling of magnetohydrodynamic effects with transparent media. That this substance may be assessed as problematic in this respect is described in Sect. 1.3, the Prandtl number of this salt mixture is 6 and thus too high to serve as a really meaningful model substance for liquid metals. The electrical conductivity given in [6] is $\sigma = 185 \text{ } \Omega^{-1} \cdot \text{m}^{-1}$. Figure 7 and Table 5 show that, also from the point

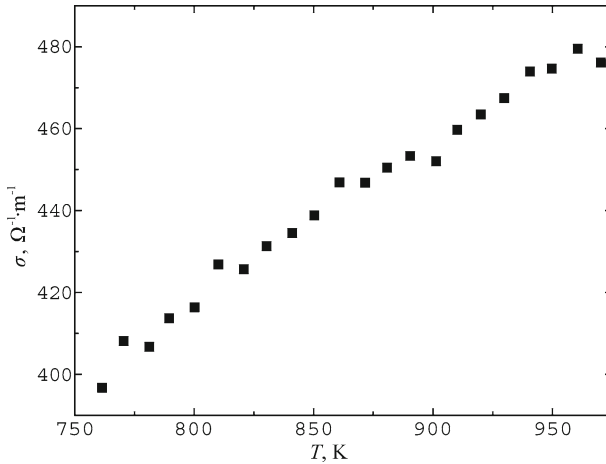


Fig. 7 Electrical conductivity σ of LiI as a function of temperature T . Measured data (*square*) suggest a linear dependence on T

of view of the maximum achievable strength of magnetohydrodynamic effects being proportional to σ , LiI outperforms LiCl–KCl.

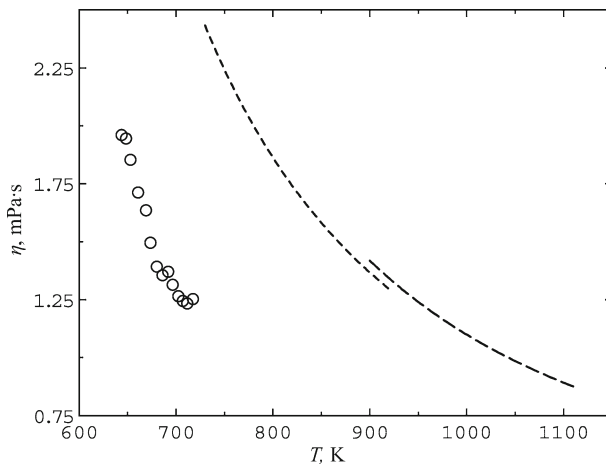
The most important, second reason to carry out measurements of σ is the need of an indicator for choosing among the vast number of combinations and concentration ratios if the expensive measurement of viscosity is required. Measuring σ is much easier and quicker than reliably measuring η . The expectation here was that the dependence of σ on T is related to that of η on T . A quite extended series of measurements (not shown here) of the systems LiBr–LiF, LiBr–LiI, and LiCl–LiI indeed exhibited an absolute minimum in the dependence of σ on the composition.

Reference [27] indicates that the viscosity of molten salt mixtures does not depend linearly on the composition. Whether the viscosity isotherms in a viscosity diagram $\eta = \eta(\text{composition})$ are convex or concave depends on the particular type of the mixture. The isotherms for alkali halides are concave. This means that the admixture of a salt having a higher viscosity compared to one with a lower viscosity does not result in a significant difference in the viscosities from the lower value to that of the mixture. The range of composition where the viscosity of the mixture does not significantly change may extend up to 40 mol% of the admixed species.

Finally, the dependence of viscosity on temperature was measured at the composition for which the electrical conductivity is a minimum. Figure 8 shows a representative result obtained with the LiCl–LiI system. Expectedly from [27], the viscosity of the mixture is higher than that of pure LiI. The range of comparable viscosity between the mixture and pure LiI does not differ significantly with temperature. The mixture reaches the low value of 1.25 mPa·s at about 700 K, whereas the LiI has to be heated to about 950 K to achieve this low value. It is worth noting that the expectation of a relationship between the viscosity and the electrical conductivity has proven to be true, at least, qualitatively.

Table 5 Measured electrical conductivity σ as a function of temperature T

T (K)	σ ($\Omega^{-1} \cdot \text{m}^{-1}$)
761.65	396.7
770.73	408.2
781.73	406.8
789.70	413.7
800.35	416.5
810.38	427.0
821.10	425.7
830.32	431.3
841.10	434.4
850.35	438.6
860.78	446.8
871.84	446.6
880.93	450.5
890.23	453.4
901.42	451.9
910.25	459.8
920.24	463.4
929.94	467.5
940.32	474.0
950.00	474.5
960.23	479.5
970.58	475.9

**Fig. 8** Comparison of the dynamic viscosity of a LiCl–LiI mixture with 64 at % LiI (circle), LiCl (line with short dashes), and LiI (line with long dashes). The curves are fitted according to Eq. 1, where the values for A and E are taken from [19] (LiCl) and are determined in the present work (LiI), respectively

4 Conclusion

The present article shows that meaningful physical modeling of liquid metal flows can be fulfilled when using a melt of lithium iodide replacing the fluid under investigation. With respect to welding processes, which are characterized by the predominance of thermocapillary effects, the requirements may be conveniently summarized as: (a) robust Marangoni effect, (b) transparency, and (c) small Prandtl number ($Pr \leq 1$). Whereas other proposed substances may satisfy one or two of these requirements, lithium iodide fulfills all of them. The first two conditions, confirmed in the present measurements of the surface tension, as well as a moderate melting temperature ensure acceptable experimental efforts. Calculation of the Prandtl number requires determination of the thermal conductivity, which is measured for the first time. Comparison with available data for other salts revealed that the thermal conductivity of lithium iodide is the highest of all alkali iodides. Uniquely among the latter and among lithium halides is an increase of the thermal conductivity with temperature. Combining our measured quantities, it is demonstrated that a Prandtl number of 1 or less is reachable which was not predictable before this work. Hence, the regime of diffusively dominated heat transport may be entered with a transparent substance for experimentally manageable temperatures. Thus, lithium iodide is a model fluid for which its thermophysical properties make it a favorable candidate for physical modeling of industrially relevant flows, particularly in the field of welding.

Acknowledgment The authors gratefully thank the “Deutsche Forschungsgemeinschaft” for financial support in the framework of the Collaborative Research Centre SFB 609.

References

1. A. Cramer, C. Zhang, G. Gerbeth, *Flow Meas. Instrum.* **15**, 145 (2004)
2. S. Eckert, A. Cramer, G. Gerbeth, Velocity measurement techniques for liquid metal flows, in *Magneto hydrodynamics—Historical Evolution and Trends*, ed. by S. Molokov, R. Moreau, H.K. Moffat (Springer, Dordrecht, 2007), pp. 275–294
3. A. Cramer, S. Eckert, V. Galindo, G. Gerbeth, B. Willers, W. Witke, *J. Mater. Sci.* **39**, 7285 (2004)
4. P. Tison, D. Camel, I. Tosello, J.J. Favier, Experimental and theoretical study of Marangoni flows in liquid metallic layers, in *Proceedings of the First International Symposium on Hydromechanics and Heat/Mass Transfer in Microgravity*, Moscow, Russia, ed. by V.S. Arduersky et al. (Gordon and Breach Science Publishers, New York, 1991)
5. J. Priede, A. Cramer, A. Bojarevičs, A.Y. Gelfgat, P.Z. Bar-Yoseph, A.L. Yarin, G. Gerbeth, *Phys. Fluids* **11**, 3331 (1999)
6. D.R. Sadoway, J. Szekely, *Metall. Trans. B* **11**, 334 (1980)
7. J.K. Koziol, D.R. Sadoway, *Mater. Res. Soc. Symp. Proc.* **87**, 173 (1987)
8. C. Limmaneevichitr, S. Kou, *Weld. J.* **79**, 126 (2000)
9. C. Limmaneevichitr, S. Kou, *Weld. J.* **79**, 231 (2000)
10. C. Limmaneevichitr, S. Kou, *Weld. J.* **79**, 324 (2000)
11. Yu. Plevachuk, V. Sklyarchuk, *Meas. Sci. Technol.* **12**, 23 (2001)
12. Yu. Plevachuk, V. Sklyarchuk, A. Yakymovych, B. Willers, S. Eckert, *J. Alloys Compd.* **394**, 63 (2005)
13. R. Roscoe, *Proc. Phys. Soc.* **72**, 576 (1958)
14. V. Sklyarchuk, Yu. Plevachuk, *Meas. Sci. Technol.* **16**, 467 (2005)
15. Yu.V. Najdich, *Contact Phenomena in Metallurgical Melts* (Naukova Dumka, Kyiv, 1972)
16. P. Kozakevitch, in *Physico Chemical Measurements at High Temperatures*, ed. by J.O.M. Bockris, J.L. White, J.D. Mackenzie (Butterworth, London, 1959), ch. 9, p. 208

17. G.J. Janz, *Molten Salts Handbook* (Academic Press, New York, 1967)
18. G.J. Janz, F.W. Dampier, G.R. Lakshminarayanan, P.K. Lorenz, R.P.T. Tomkins, *Molten Salts*: vol. 1, *Electrical Conductance, Density, and Viscosity Data* (U.S. Department of Commerce, 1968)
19. G.J. Janz, C.B. Allen, N.P. Bansal, R.M. Murphy, R.P.T. Tomkins, *Physical Properties Data Compilations Relevant to Energy Storage. II. Molten Salts: Data on Single and Multi-Component Salt Systems* (U.S. Department of Commerce, 1979)
20. N. Nakazawa, Y. Nagasaka, A. Nagashima, *Int. J. Thermophys.* **13**, 763 (1992)
21. Y. Nagasaka, N. Nakazawa, A. Nagashima, *Int. J. Thermophys.* **13**, 555 (1992)
22. I.G. Kipov, S.N. Zadumkin, A.I. Temporov, *Zh. Fiz. Khim.* **44**, 2618 (1970)
23. M.V. Smirnov, V.P. Stepanov, Physical chemistry and electrochemistry of molten and solid electrolytes, in *Structures and Properties of Electrolytes* (Reports of All-Union Conference, Sverdlovsk, USSR, 1973)
24. M.V. Smirnov, V.P. Stepanov, *Electrochim. Acta* **27**, 1551 (1982)
25. Private communication, V. Mekhonoshin, V. P. Stephanov, including the mention of the obviously unavailable book “*Mezhfaznye yavleniya v ionnykh solevykh rasplavakh*, UIF ‘Nauka’, Yekaterinburg, 1993” (Moscow, 2007)
26. I.G. Murgulescu, C. Telea, *Rev. Roum. Chim.* **22**, 683 (1977)
27. A.I. Beljajew, E.A. Shemtschushina, I.A. Firsanova, *Physikalische Chemie geschmolzener Salze* (VEB Deutscher Verlag für Grundstoffindustrie, Leipzig 1964), ch. 3, pp. 106–198